CALCULATION OF TOTAL CROSS SECTIONS FOR CHARGE EXCHANGE IN MOLECULAR COLLISIONS

NASA RESEARCH GRANT NO. 1361

FINAL REPORT

31 December 1979

(NASA-CR-162560) CALCULATION OF TOTAL CROSS SECTIONS FOR CHARGE EXCHANGE IN MOLECULAR COLLISIONS Final Report (Xavier Univ. of Louisiana, New Orleans.) 32 p HC A03/MF A01 CSCL 20H G3/72

N80-14879

Unclas 46532

Juliette Ioup
Principal Investigator
Physics/Pre-Engineering Department
Xavier University
New Orleans, LA 70125
(504)486-7411 ext 341, 241

CALCULATION OF TOTAL CROSS SECTIONS FOR CHARGE EXCHANGE IN MOLECULAR COLLISIONS

Contents

Introduction	3
Molecular Charge Exchange in Nitrogen	3
Gas-Surface Charge Transfer Collisions	5
Trace Gas Identification	8
The Quadrupole Mass Spectrometer	8
The 127° Cylindrical Electrostatic Analyzer	16
Deconvolution of Mass Spectrometer Data	21
Iterative Method	26
Fourier Transform Related Method	26
Mass Spectrometer Data	26
Footnotes	29
Publications, Talks, Conference	31
Books Purchased, Equipment Purchased	32

CALCULATION OF TOTAL CROSS SECTIONS FOR CHARGE EXCHANGE IN MOLECULAR COLLISIONS

Introduction

Several varied activities were completed during the time period of this grant. As the needs and interests of the associated NASA research personnel changed, the direction of the research under this grant also changed. Areas of investigation included nitrogen ion-nitrogen molecule collisions; molecular collisions with surfaces; molecular identification from analysis of cracking patterns of selected gases; computer modelling of a quadrupole mass spectrometer; study of space charge in a quadrupole; transmission of the 127° cylindrical electrostatic analyzer; and mass spectrometer data deconvolution. Each of these areas will be briefly summarized below. More detailed reports are contained in the various status reports submitted during the grant period.

A list of the publications submitted under this grant is attached. Talks given related to this research and relevant conferences attended are listed. Books and equipment purchased with funds from this grant are also given on an attached page.

Molecular Charge Exchange in Nitrogen

A theoretical investigation of low energy collisions

of nitrogen ions with nitrogen molecules was made using the multistate impact parameter method of Flannery, Cosby, and Moran.[1] The method[2] attempts to take into account the vibrational states of the incident ions and of the products, with the target neutral molecules assumed to be initially in the ground state. Total cross sections for N_2^+ on N_2 were obtained. Energies were such that electronic and vibrational states were calculated, while rotational states were neglected.

The charge-transfer process in diatomic nitrogen is resonant and symmetric so that the wavefunction may be expanded in terms of the gerade and ungerade eigenfunctions for each electronic state of the quasimolecular complex formed. In order to include nonresonant channels, the wavefunction is expanded in terms of the molecular eigenfunctions of the unperturbed Hamiltonian for the isolated molecular systems. This expansion is substituted into the time-dependent Schrodinger wave equation for the internal coordinates and the charge-transfer total cross section derived. The interaction potential is assumed to be spherically symmetric and can be obtained from the gerade-ungerade splitting of the vibrational motion. A Morse function[3] is used for the gerade potential, and with the modified Lennard-Jones potential[4,5] gives the interaction energy for the gerade state for this reaction. The ungerade potential is given by Sato.[6]

Vibrational overlaps are needed in order to obtain the transition amplitudes for the charge-transfer cross section. Flanner et al[1,7] found that the excitation defects occurred in groups or "bands" separated by approximately one vibrational

quantum of energy. Therefore the channels could be considered to be degenerate within a given band, greatly simplifying the calculations involved. The charge transfer cross sections were obtained by numerical integration.

The low-velocity approximation[2] can be used for collisions in which the incident velocity is small enough so that the excitation defect is approximately zero. Some representative results of both the low-velocity approximation and the full multistate treatment as well as some additional experimental data from the literature are presented in Figs. 1 and 2 for comparison with the Langley data. Calculations were made for the cases where the incident ion, target neutral, and products were all in the ground electronic state. The vibrational states for the incident ion were the ground and the first three excited states; for the target teutral, the ground state; and for the products, the ground and first two excited states.

Gas-Surface Charge Transfer Collisions

The suitability of the multistate impact parameter method to gas-gas/surface and gas-surface charge transfer collisions was studied.[8-10] It was concluded that although this method had direct application to the molecular nitrogen collisions, extension to collisions where surfaces are present would involve time and effort greater than could be justified at the present time.

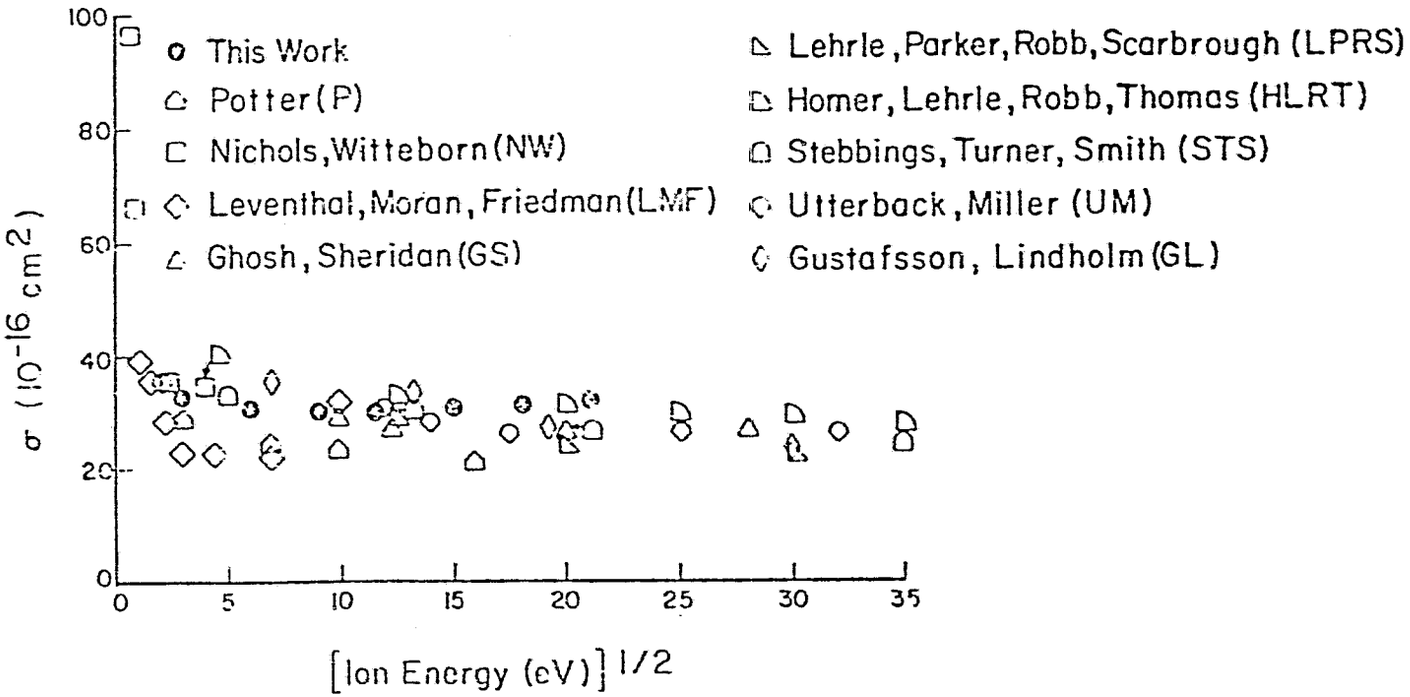

Figure 1. Comparison σ This Work with Experimental Results of Others.

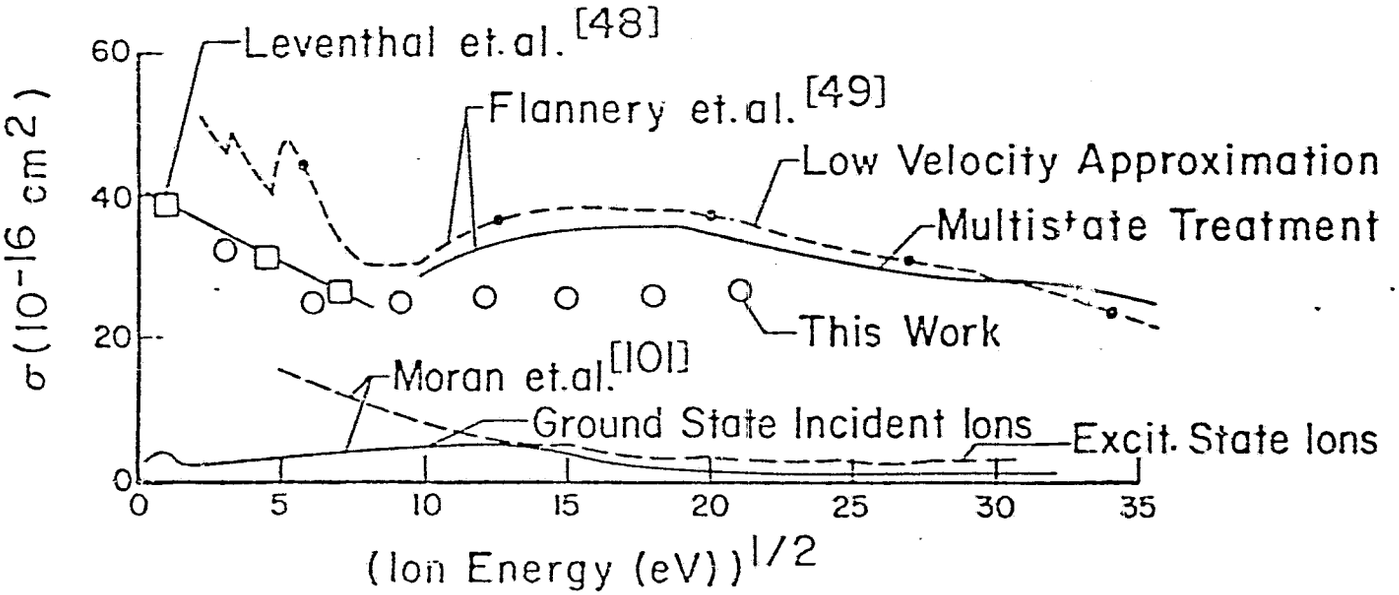

Figure 2. Comparison σ This Work with Theoretical Calculations of Others.

Trace Gas Identification

Computer programs were constructed to identify trace gases from data from a mass spectrometer designed for the Space Shuttle. Mass peak data for 149 chemical compounds were obtained from the data bank of the Cyphernetics Corporation of Ann Arbor, Michigan, via an acoustic coupler on the telephone line. Cracking patterns for each compound were sorted by computer which then was programmed to print out peak height, name, total mass, and allowable parts per million for those which had fragment peaks at each atomic mass number from 1 to 207. This list was then searched and data output for those mass numbers for which there was only one compound fragment present, only two, etc. This type of information can be used in programming the computer for the Shuttle mass spectrometer to identify positively and uniquely the compounds which may be present in the sampled gases.

The Quadrupole Mass Spectrometer

In order to investigate molecular collisions experimentally, it is often necessary to select ions for mass and energy before the collision and to analyze the same properties after. This may be accomplished by means of a mass spectrometer and/or energy analyzer. A computer model of the quadrupole mass spectrometer was used to investigate its properties. Fig. 3 gives the geometry of a quadrupole mass spectrometer.[11-13]

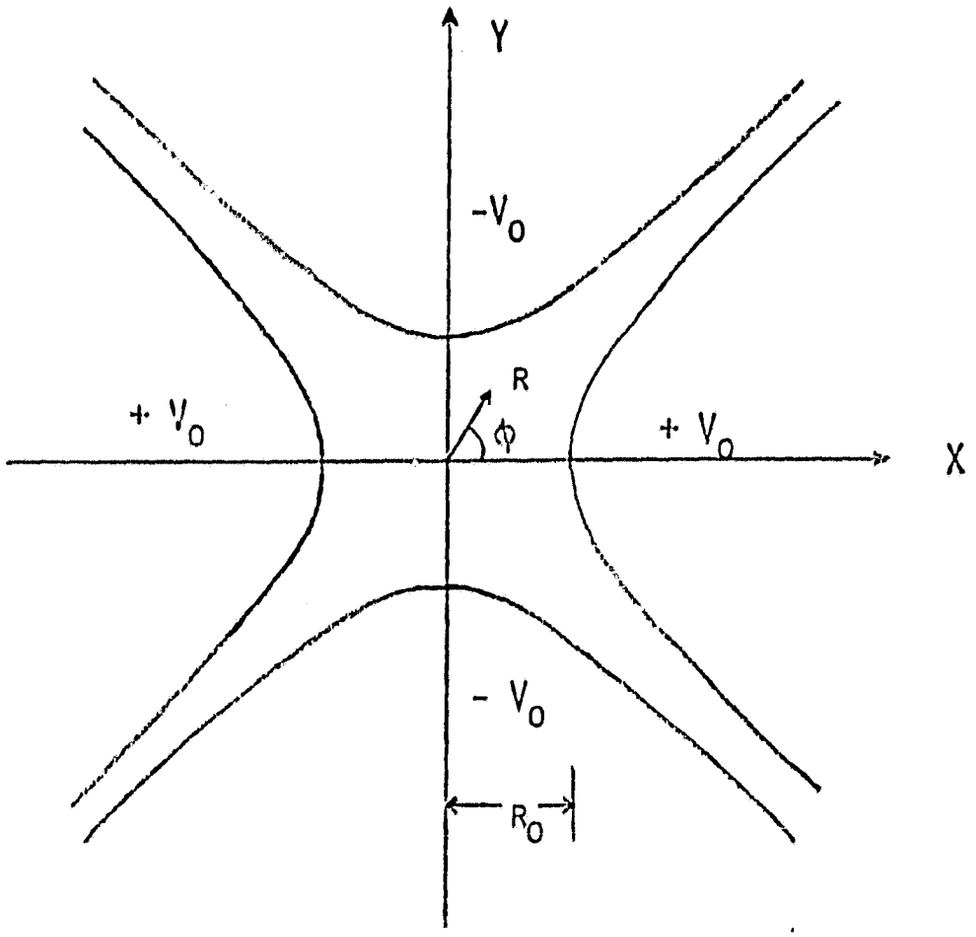

QUADRUPOLE MASS SPECTROMETER - END VIEW

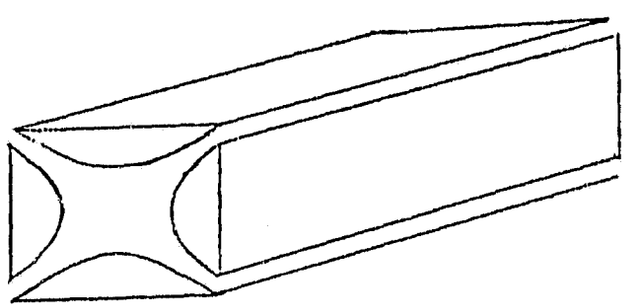

QUADRUPOLE MASS SPECTROMETER - SIDE VIEW

Figure 3. Geometry of the Quadrupole Mass Spectrometer.

The differential equations of motion (the Mathieu equations) in cylindrical coordinates for an ion passing through a quadrupole were solved by a computer code using a fourth-order Runge-Kutta method based on Fehlberg's formulas.[14] Fig. 4 shows the region of stability for a quadrupole. The operating quantities A and Q are related to the direct current and radio frequency voltages on the pole pieces.[11] The path of an ion can be followed through the quadrupole to determine its position and velocity at any instant by the computer program. The position,speed, and phase of the incident ions were varied to simulate an ion beam entering the quadrupole, and transmission curves were calculated for selected beams. The position and velocity can be determined for those ions exiting, or the location where the ions struck the quadrupole rods for those not transmitted.

Fringing fields at the entrance and exit of the quadrupole greatly influence the ion path. In an attempt to reduce the effect at the entrance, it was proposed to test a quadrupole in which the pole pieces were aligned in a geometry resembling a funnel, with the entrance larger than the exit. Computer programs were developed so that path-dependent boundary conditions could be specified corresponding to different pole separations at the entrance and exit. Transmissions were calculated for various geometries of the quadrupole. For a 20 pi trajectory, resolution of 100, with ions entering in an annular ring parallel to the quadrupole axis, it was found that increasing the quadrupole entrance radius caused the width of the transmission peak to decrease, as shown in

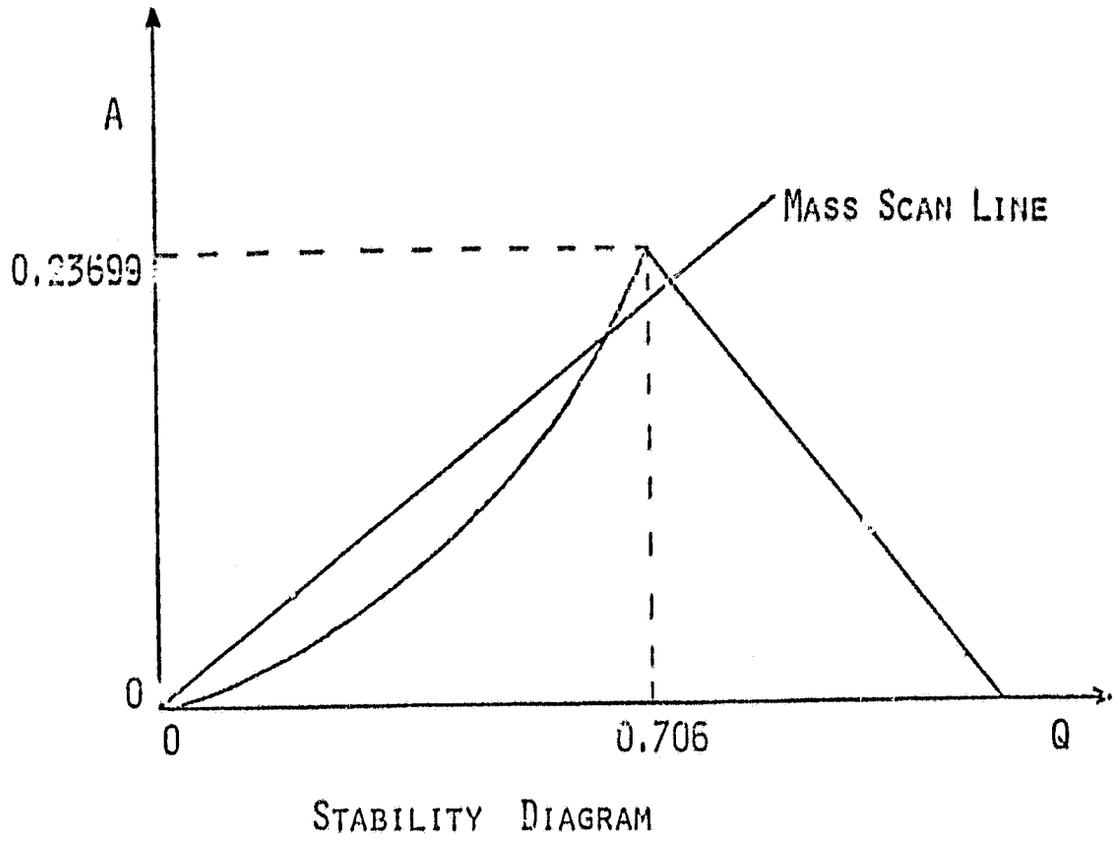

Figure 4. Stability region for the quadrupole mass spectrometer.

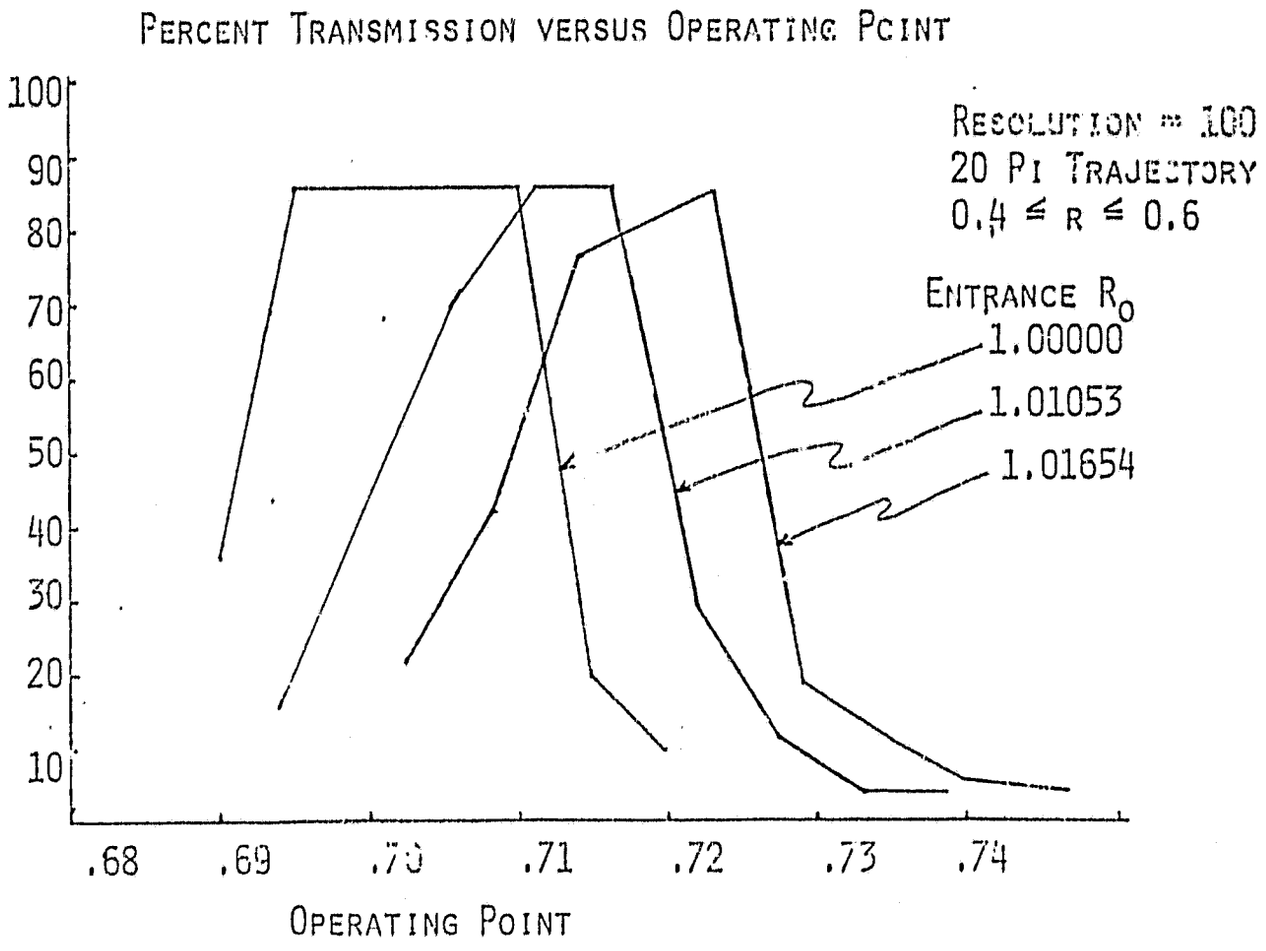

Figure 5. Transmission of a quadrupole mass spectrometer.

Figs. 5 and 6. Similar curves are given in Fig. 7 for a resolution of 500. Transmission peaks for a 20 pi trajectory with the ions entering in an annular ring parallel to the quadrupole axis for non-slanted pole pieces are given in Fig. 8.

In order to investigate the space charge buildup inside a quadrupole mass spectrometer, the behavior of an electron in a quadrupole was investigated. The differential equations of motion for an electron in the quadrupole were solved and various paths plotted. Calculations were performed for the NASA Gas Analysis and Detection System (GADS). It was found that a large fraction of off-axis electrons entering the quadrupole under the given conditions would strike the rods.

The time which any charged particle spends in a quadrupole mass spectrometer was obtained as a function of mass. Numerical values were computed for an electron and for singly-charged ions of various masses introduced into the GADS quadrupole.

Charged particles passing from the ion source into the quadrupole field region in the GADS must pass through small circular holes in plates held at various potentials. The electric field and the potential for such a geometry were determined for points on an axis passing through the center of the circular hole. The electric field and the potential were also obtained for points in the plane of the opening inside the circle using Laplace's equation, Gauss's Law, and Ohm's Law. The resulting computed numerical values were compared with experimental data obtained at NASA-Langley.

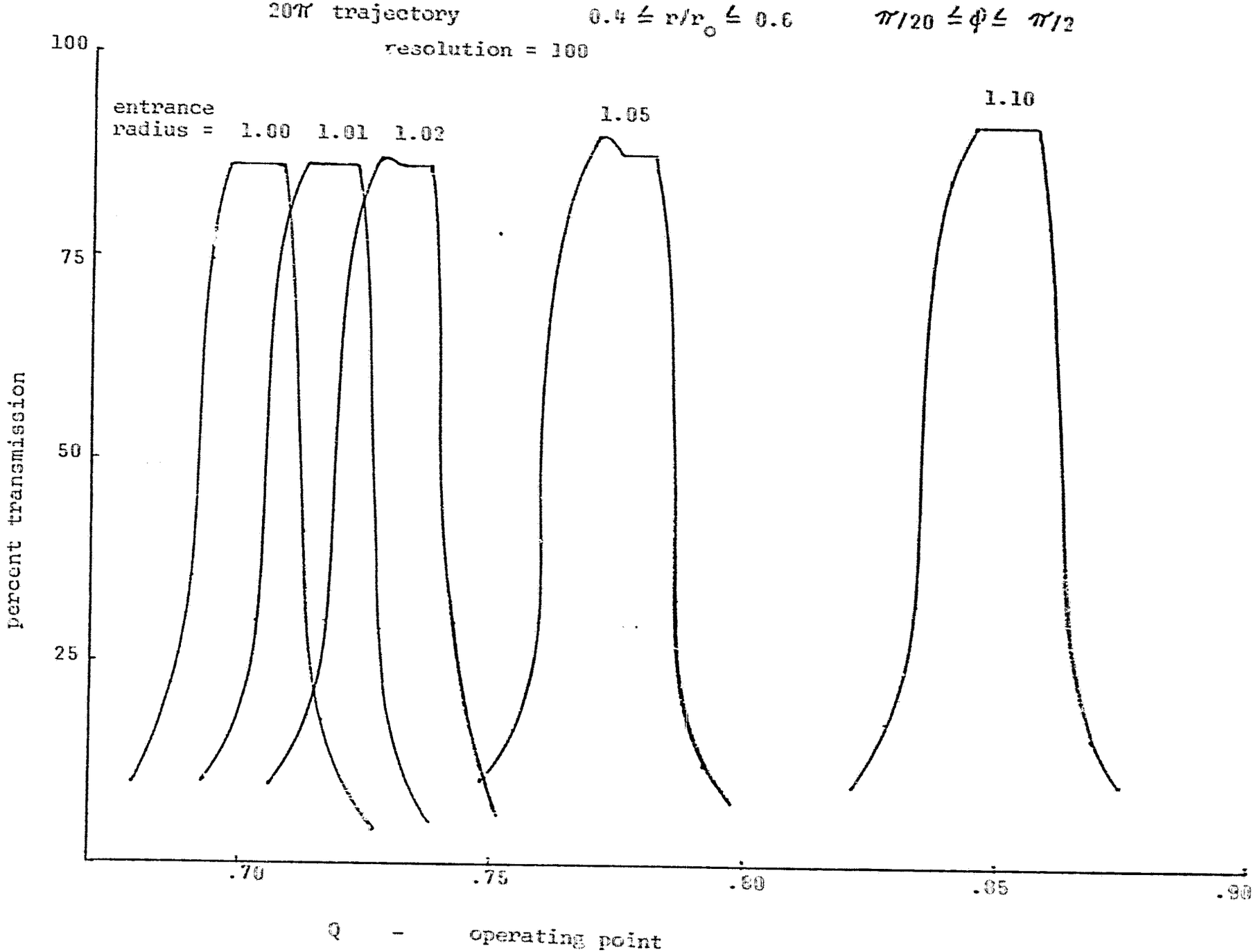

Figure 6. Transmission of a quadrupole mass spectrometer.

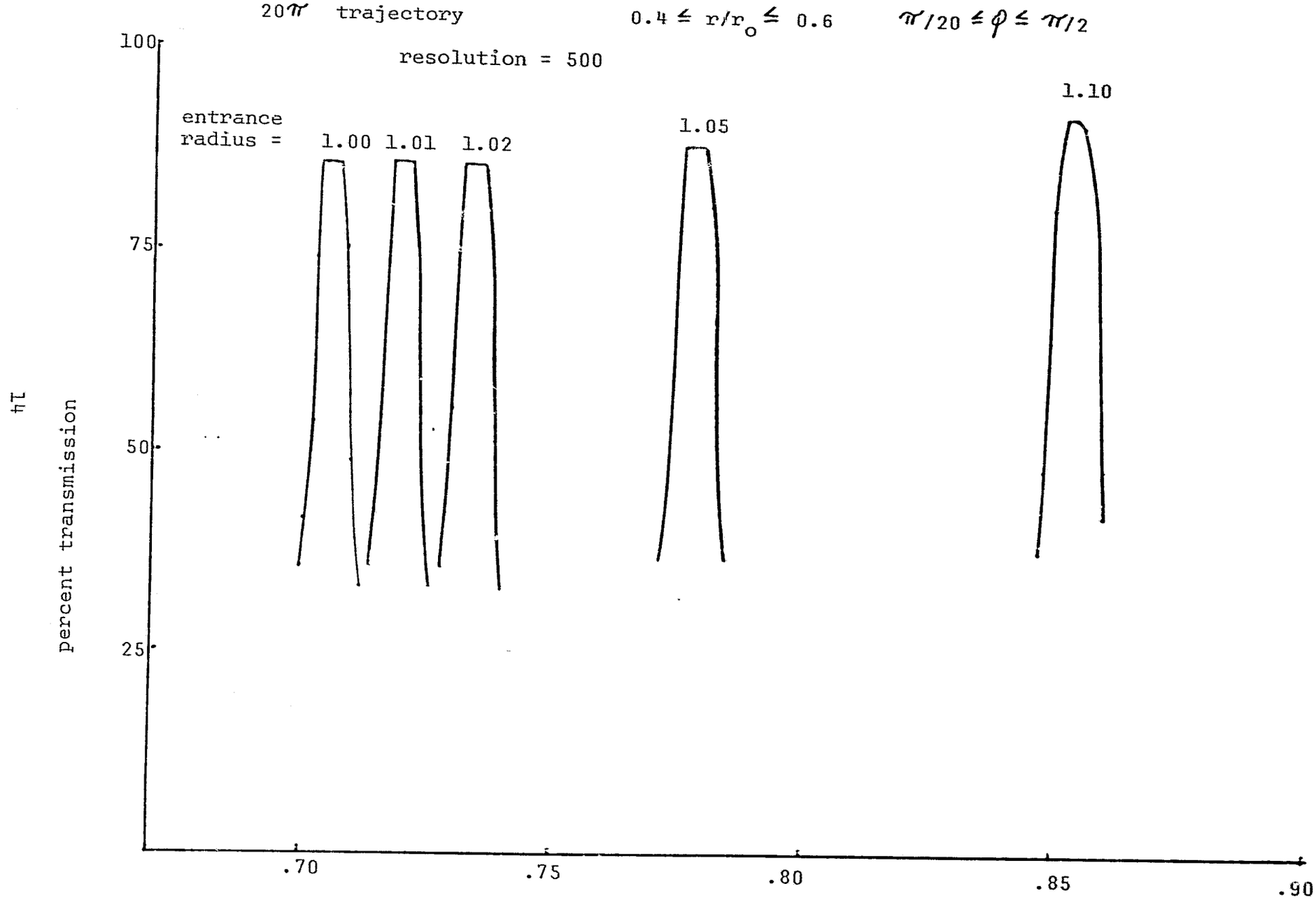

Figure 7. Transmission of a quadrupole mass spectrometer.

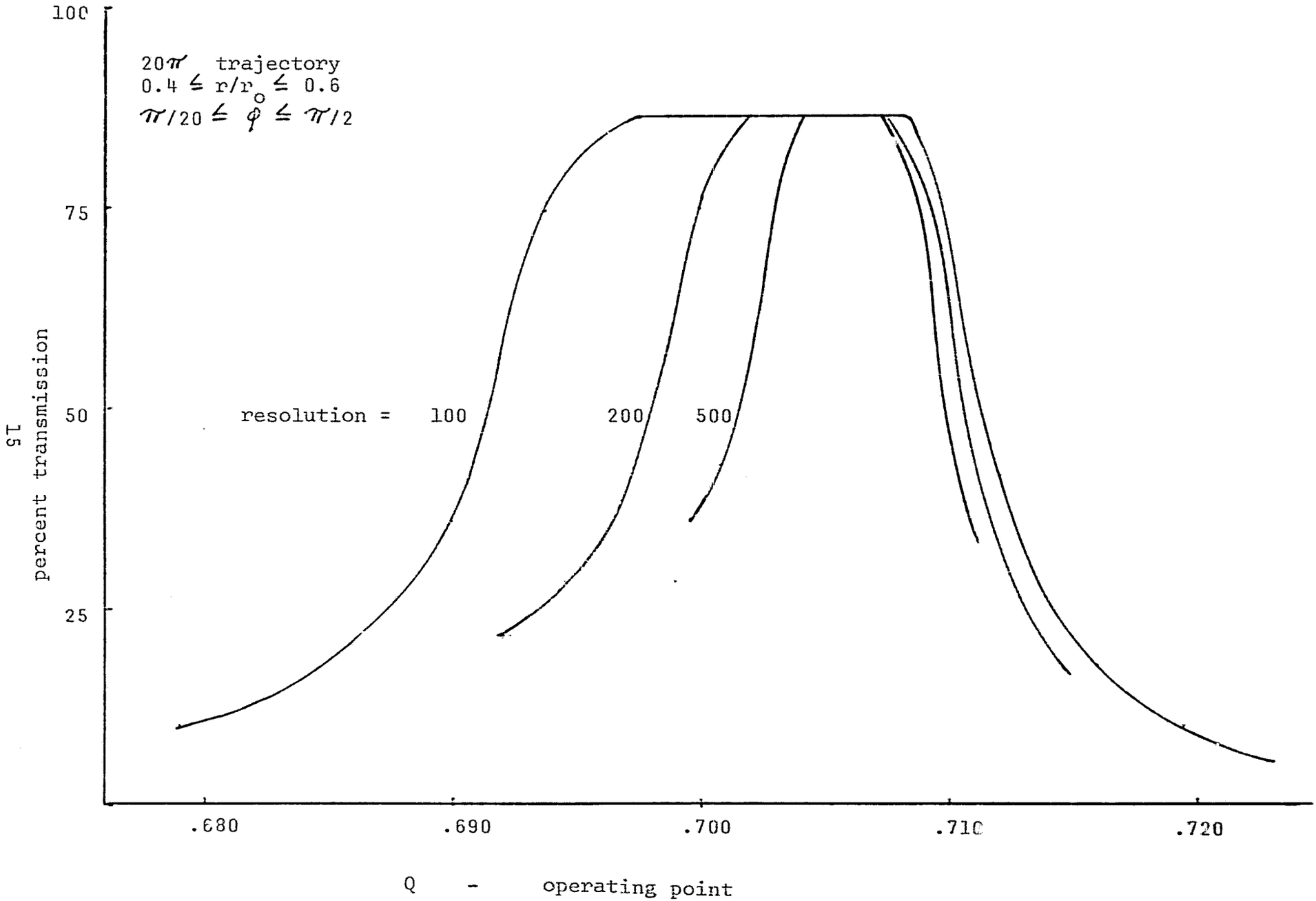

Figure 8. Transmission of a quadrupole mass spectrometer with parallel pole pieces.

The 127° Cylindrical Electrostatic Analyzer

The theory of the transmission of particles through the 127° cylindrical electrostatic analyzer[15,16] was studied. The geometry of such an analyzer is shown in Fig. 9. Analytical expressions for the analyzer and low-current selector transmissions as functions of energy and two input angles, in and out of the plane of incidence, were obtained. A uniform distribution of particles across the entrance slit was assumed to obtain analytical expressions for the response functions for a given angle for the 127° cylindrical electrostatic analyzer for analyzer geometries in which the entrance slit is smaller than, equal to, or larger than the exit slit. The resolution and the magnification of the analyzer considered as an electron lens were also obtained. Results of this study may be used to aid the choice of analyzer design parameters and to study optimization of the analyzer.

The effective response function for the 127° cylindrical electrostatic analyzer was obtained as a function of incident particle energy from the response function by assuming a uniform distribution in incident angle. Separate analytical expressions are given in Figs. 10-12 for the effective response functions for analyzer geometries in which the entrance slit is smaller than, equal to, or larger than the exit slit. Output curves for the 127° analyzer used as an energy selector (monochromator) and as an energy analyzer were obtained for input distributions which were Gaussian in energy. Shifts in peak energy of the selector and analyzer output curves

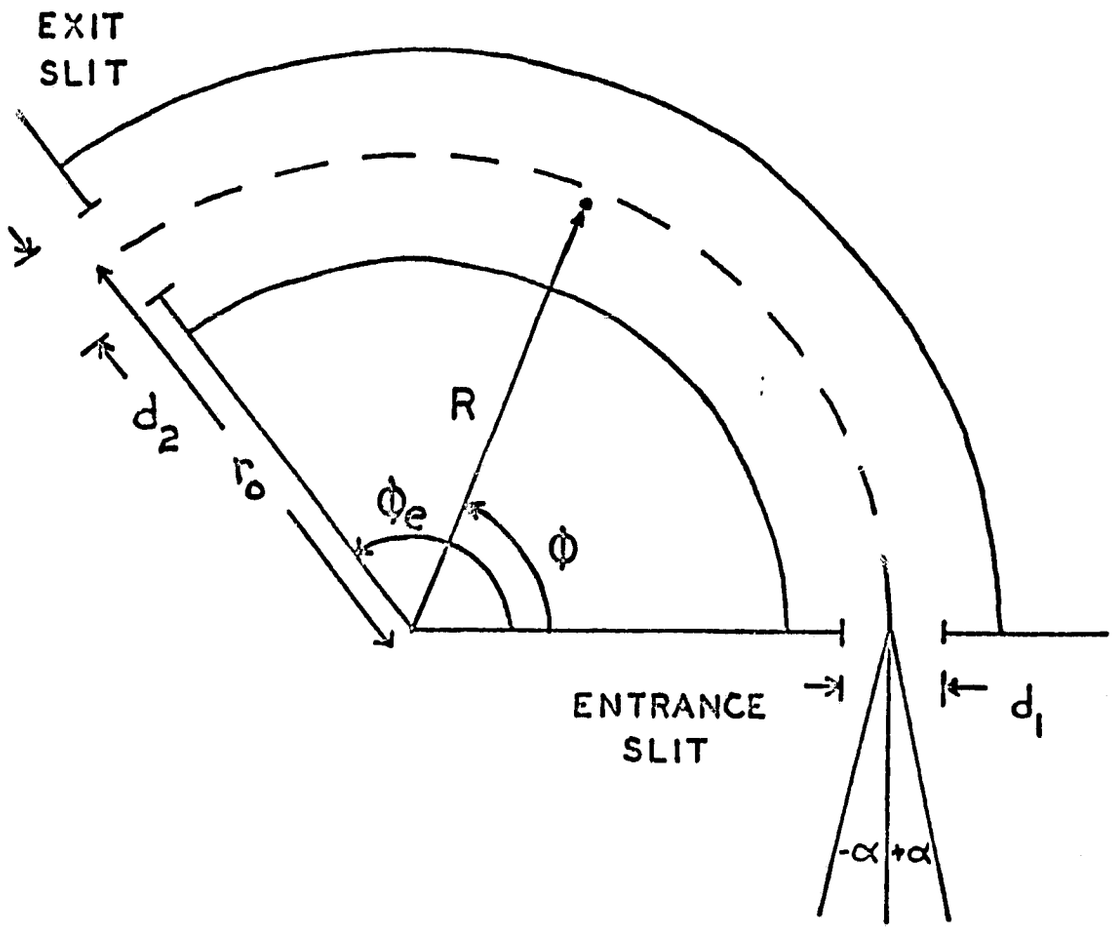

Figure 9. Geometry of the 127° cylindrical electrostatic analyzer, showing coordinates and angles.

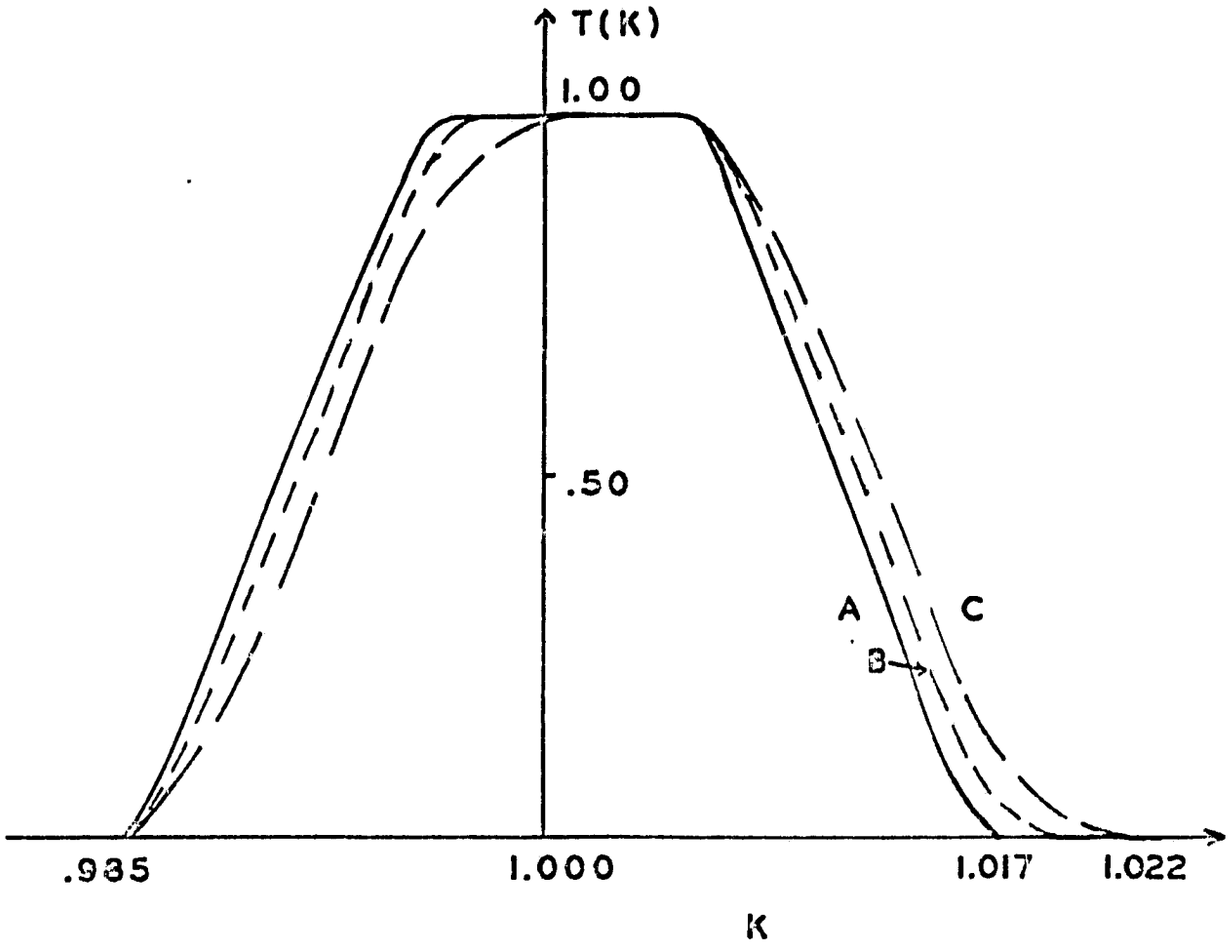

Figure 10. The effective response function T(k) versus relative energy k. Entrance slit = .01 r_o, exit slit = .02 r_o. Curve A for $\alpha_o = 2^o$, B for 3^o, and C for 4^o.

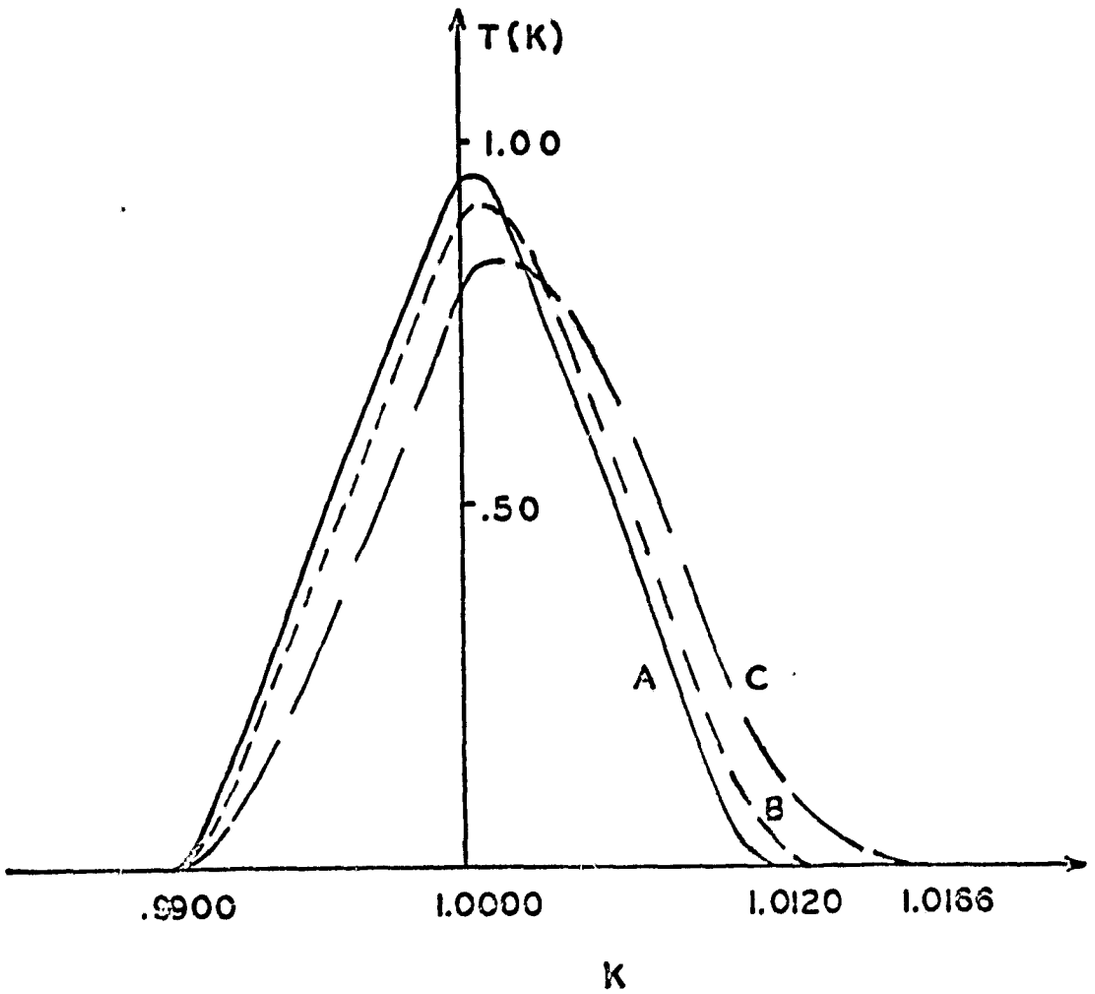

Figure 11. The effective response function T(k) versus relative energy k. Entrance slit = exit slit = .01 r_o. Curve A for $\alpha_o = 2^o$, B for 3^o, and C for 4^o.

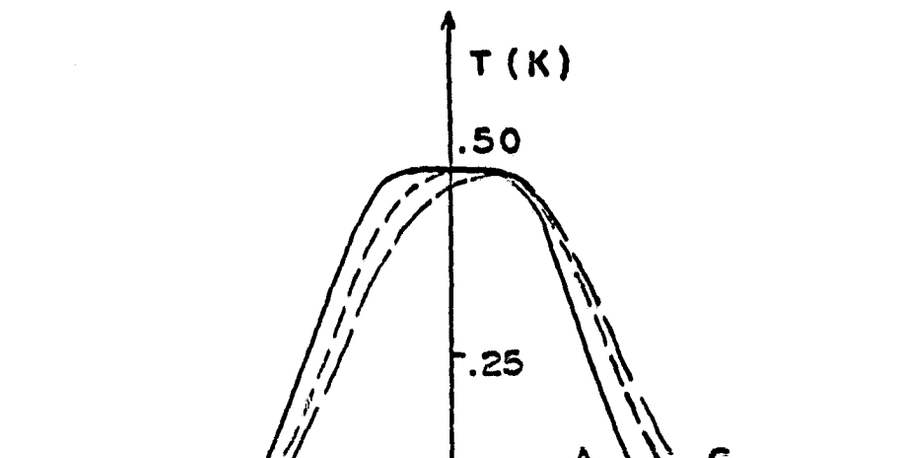

Figure 12. The effective response function T(k) versus relative energy k. Entrance slit = .01 r_o, exit slit = .005 r_o. Curve A for $\alpha_o = 2^o$, B for 3^o, and C for 3.5^o.

were calculated as a function of incident angular breadth and slit width. Broadening effects and resolutions were calculated for several representative cases. Broadening curves for the three representative geometries are given in Figs. 13-15. Fig. 16 presents broadening curves for an analyzer with equal entrance and exit slits.

Deconvolution of Mass Spectrometer Data

The accuracy of any physical measurement is limited by the instruments performing it. Preliminary investigations of the mathematical technique of deconvolution for data enhancement were made. One of the advantages of this kind of computer treatment of data is that costly modifications to instruments are avoided. The deconvolution techniques of iteration and a Fourier-transform-related method were studied. Data from a magnetic mass spectrometer was used for initial testing.

Let h represent the observed distribution of data, f the true or ideal distribution, and g the apparatus or instrument function. These quantities are related according to the expression

$$h = f * g$$

where the asterisk represents the convolution of f with g:

$$h(x) = f * g = \int_{-\infty}^{\infty} f(y)\, g(x-y)\, dy$$

Physically this means that the ideal or true data describing the physical process, f, is smeared out or broadened by the measuring instrument or response function, g, to pro-

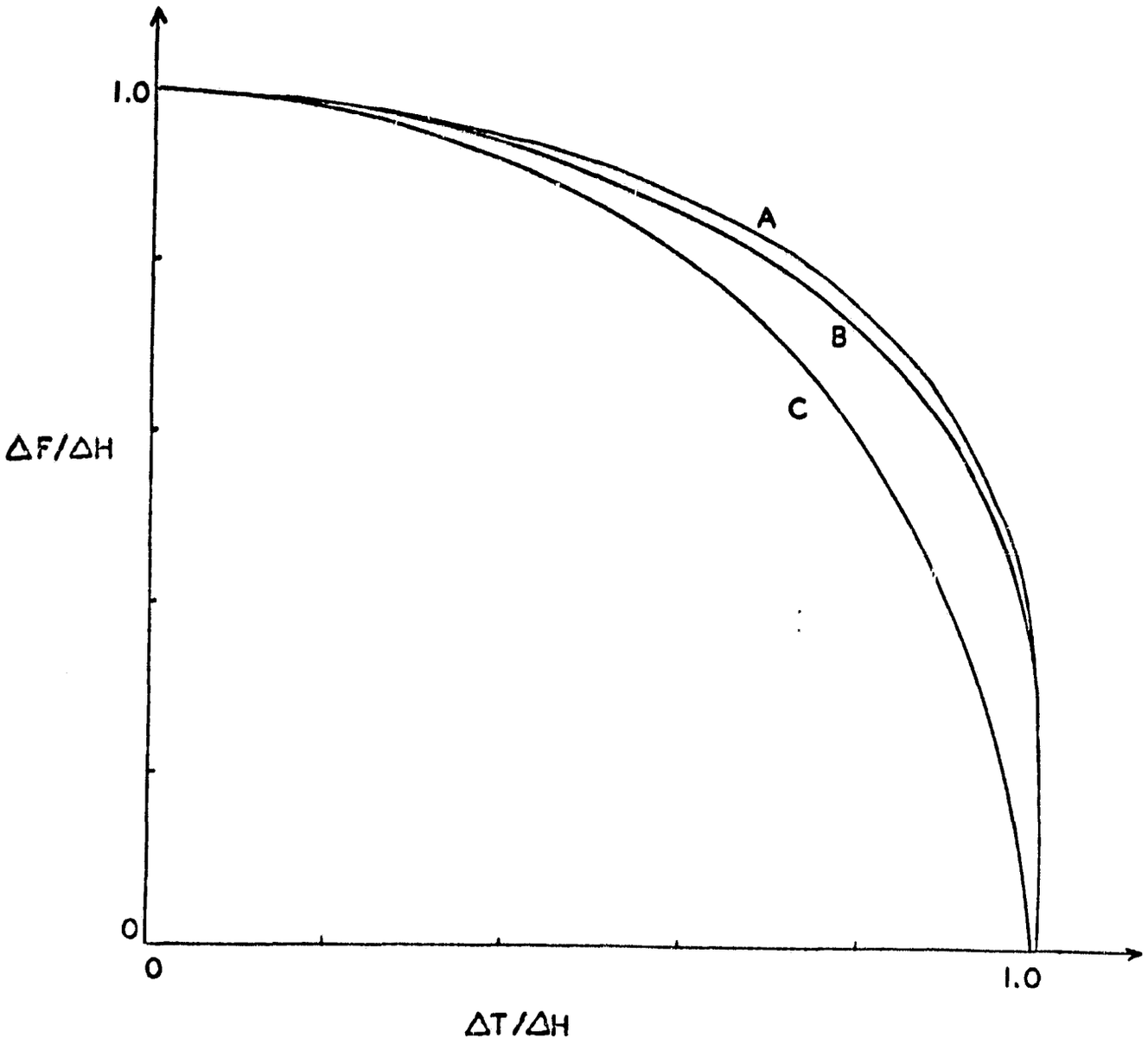

Figure 13. Broadening curves for entrance slit = .01 r_o, exit slit = .02 r_o. ΔF is the full width at half maximum (FWHM) of the input distribution in energy which is Gaussian in form, ΔT is the FWHM of the response function, and ΔH is the FWHM of the output energy distribution. Curve A for $\alpha_o = 2^o$ and B for 4^o. Curve C shows the broadening curve obtained by assuming the response function to be a Gaussian.

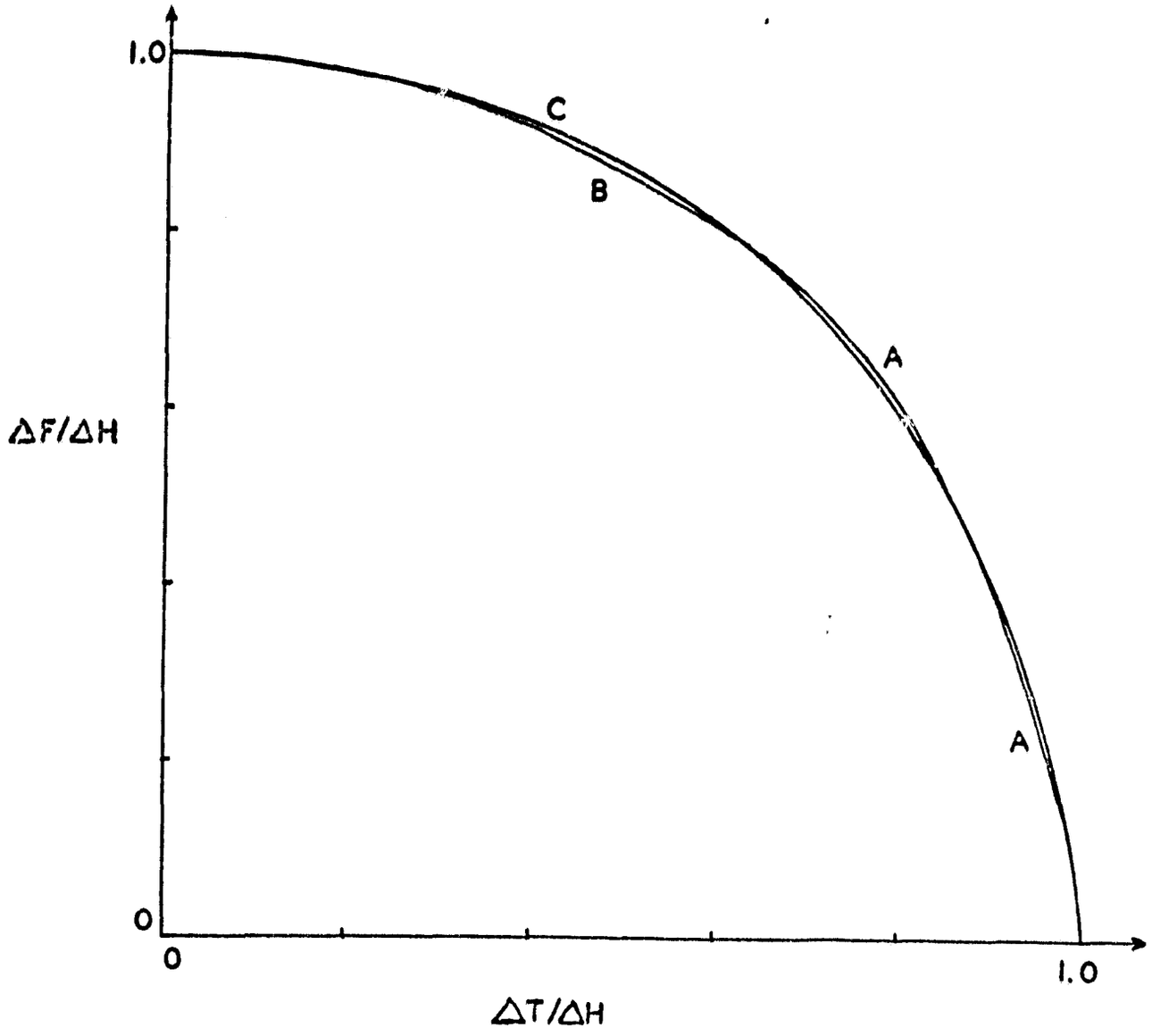

Figure 14. Broadening curves for entrance slit = exit slit = .01 r_o. ΔF, ΔT, and ΔH as defined for Fig. 13. Curve A for $\alpha_o = 2^o$ and B for 4^o. Curve C shows the broadening curve obtained by assuming the response function to be a Gaussian.

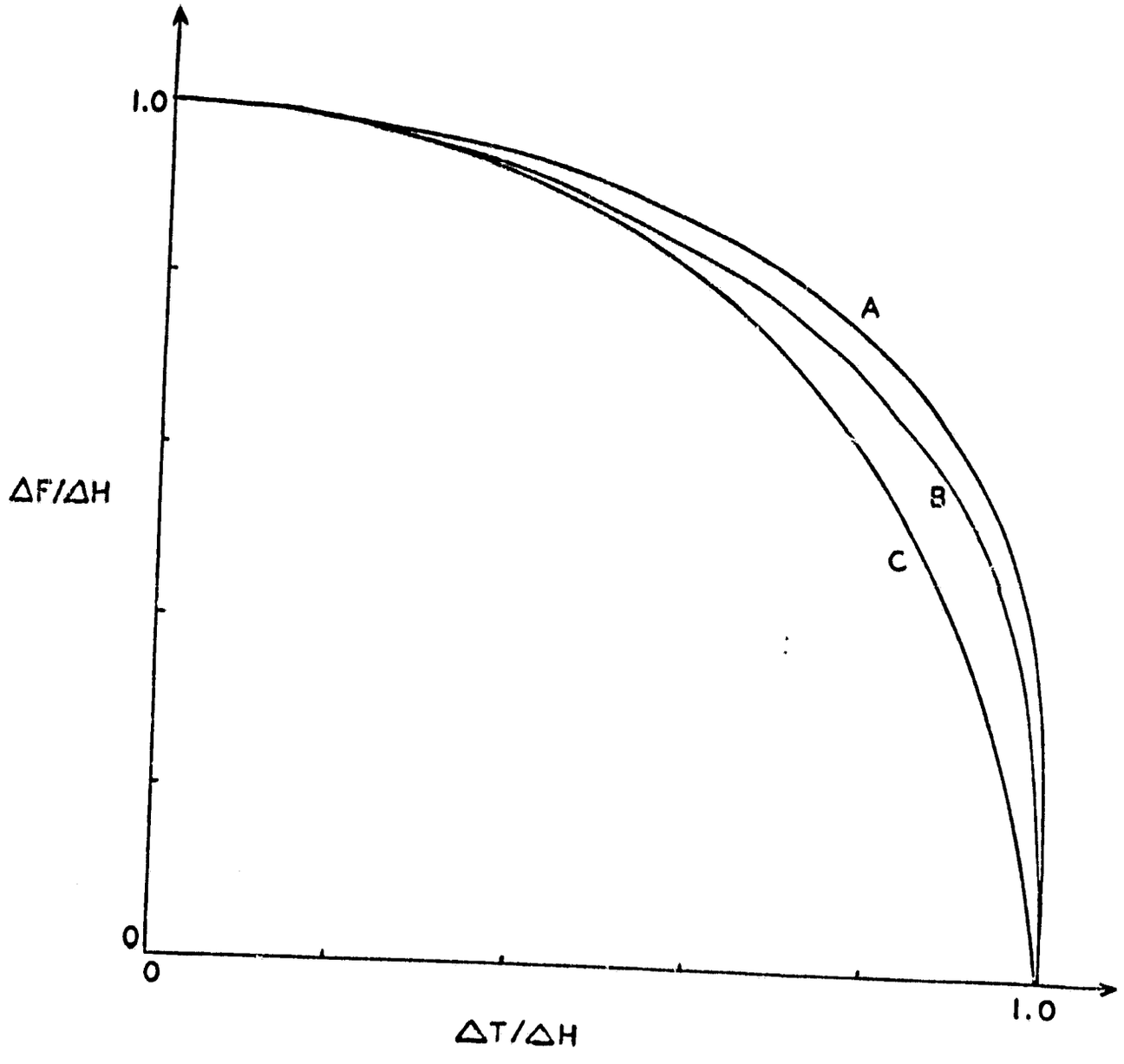

Figure 15. Broadening curves for entrance slit = .01 r_o and exit slit = .005 r_o. ΔF, ΔT, and ΔH as defined for Fig. 13. Curve A for $\alpha_o = 2^o$ and B for 3.5^o. Curve C shows the broadening curve obtained by assuming the response function to be a Gaussian.

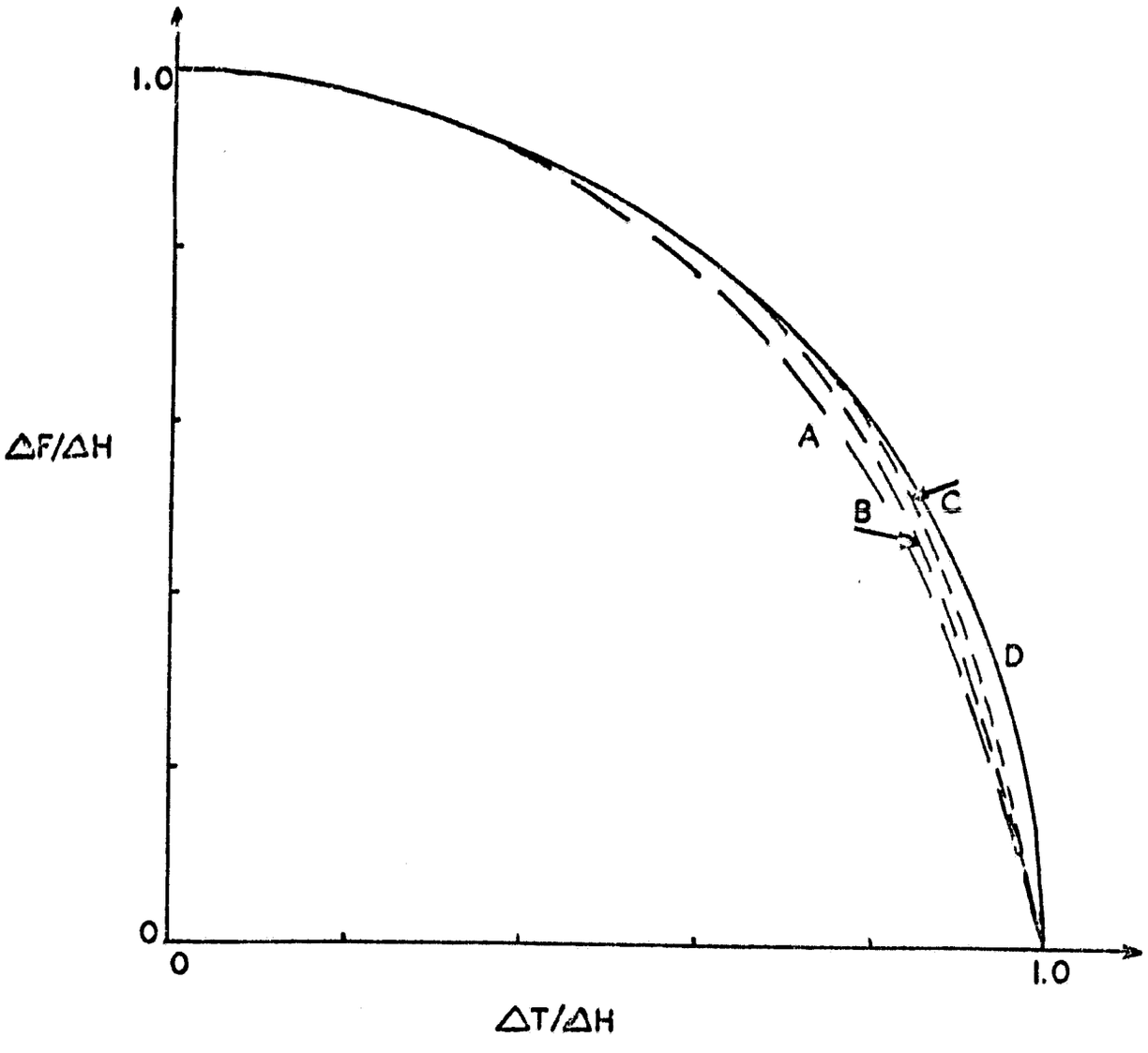

Figure 16. Broadening curves for equal entrance and exit slits for limiting input angle $\alpha = 3^{\circ}$. ΔF, ΔT, and ΔH as defined for Fig. 13. Curve A for slits of .005 r_o, B for .01 r_o, and C for .10 r_o. Curve D shows the broadening curve obtained by assuming the response function to be a Gaussian.

duce the data which is actually observed by the experimenter, h. The problem is to remove the instrument effects and obtain the ideal f from the measured h. Mathematically this corresponds to solving a Fredholm integral equation of the first kind with a difference kernel.

Iterative Method

Morrison's iterative noise removal or smoothing technique[17-19] treats the data by first smoothing it, then iteratively restoring the non-noisy output and the compatible noise. It was designed specifically to prepare data for deconvolution. The initial smoothing produces data h_1:

$$h_1 = h * g$$

The nth restoration is given by

$$h_n = h_{n-1} + (h - h_{n-1}) * g \qquad n > 1$$

After the data is smoothed and then restored the desired amount, van Cittert's iterative deconvolution or unfolding method[18-22] may be applied. The first unfolded f is assumed to be the same as h:

$$f_o = h$$

while the nth unfolding is given by

$$f_n = f_{n-1} + (h - f_{n-1} * g)$$

Fourier Transform Related Method

The Fourier transform may be used to deconvolve data because the convolution in the function domain

$$h = f * g$$

becomes a simple multiplication in the Fourier transform domain according to the convolution theorem.[17-21,23] Let

the Fourier transforms be represented by capital letters, i.e., the Fourier transform of f is F, etc. Then the equation in the Fourier domain corresponding to the convolution in the function domain is

$$H = F G$$

Rearranging this equation shows that F may be obtained by

$$F = H / G$$

if G is not zero. The inverse Fourier transform is then computed to obtain f. This is called the straightforward deconvolution solution. For discrete data, if a standard fast Fourier transform[24-25] program is used, the number of Fourier transform points computed is an integral power of two. Because noise predominates at high frequencies, only the low frequency values are used to calculate f. The higher ones above a cutoff frequency are set to zero.

The results obtained from the straightforward deconvolution described above may be enhanced by the technique of function domain fitting.[26] An artificial function, a, is constructed from the function f obtained from straightforward deconvolution and its Fourier transform A obtained. The Fourier coefficients of A and F are compared. Since noise tends to dominate the signal more at high frequencies, the high frequency coefficients of F, which are mainly determined by noise in the data, are replaced with the high frequency coefficients of A, which are not affected by noise.

Mass Spectrometer Data

Mass spectrometer data is usually presented in the form

of mass peaks, that is, the percent transmission of the ions plotted versus mass. The peak height or more generally the area under the peak is proportional to the relative abundance of that mass. If there is any overlap of the peaks, peak location and area (or height) will be correspondingly in error. Therefore it is desirable to unfold the overlapping peaks to obtain completely resolved peaks to pinpoint accurately the peak location for mass determination and peak area (or height) for relative abundance information.

Mass spectrometer data may contain two or more overlapping mass peaks. Preliminary investigation of the resolution of these smeared peaks was made, with encouraging results. This research will be continued under another NASA grant.

Footnotes

1. M. R. Flannery, P. C. Cosby, and T. F. Moran, J. Chem. Phys. 59, 5494 (1973)

2. S. N. Ghosh and W. F. Sheridan, J. Chem. Phys. 27, 1436 (1957)

3. R. F. Potter, J. Chem. Phys. 22, 974 (1954)

4. R. F. Stebbing, B. R. Turner, and A. C. H. Smith, J. Chem. Phys. 38, 2277 (1963)

5. N. G. Utterback and G. H. Miller, Rev. Sci. Instr. 32, 1101 (1961)

6. H. W. Berry, Phys. Rev. 74, 848 (1948)

7. T. F. Moran, K. J. McCann, and M. R. Flannery, J. Chem. Phys. 63, 3857 (1975)

8. F. O. Goodman and H. Y. Wachman, Dynamics of Gas-Surface Scattering, Academic Press, 1976

9. M. Prutton, Surface Physics, Clarendon, 1975

10. J. R. Woodyard, Low Energy Sputtering Studies, Ph.D. Dissertation, University of Delaware, 1966

11. P. H. Dawson, ed., Quadrupole Mass Spectrometry and Its Applications, North Holland, 1976

12. P. W. Hawkes, Quadrupoles in Electron Lens Design, Academic Press, 1970

13. A. Septier, ed., Focusing of Charged Particles, Vol. I, Academic Press, 1967

14. M. Mosharrafa, NASA Technical Report, 1970

15. A. L. Hughes and V. Rojansky, Phys. Rev. 34, 284 (1929)

16. A. L. Hughes and J. H. McMillen, Phys. Rev. 34, 291 (1929)

17. J. D. Morrison, J. Chem. Phys. 39, 200 (1963)

18. G. E. Ioup and B. S. Thomas, J. Chem. Phys. 46, 3959 (1967)

19. G. E. Ioup, Analysis of Low Energy Atomic and Molecular Collisions: Semi-classical Elastic Scattering Calculations and Deconvolution of Data, Ph.D. Dissertation, University of Florida, 1968

B. R. Frieden, Image Enhancement and Restoration, in T. S. Huang, ed., Picture Processing and Digital Filtering, Vol. 6, Topics in Applied Physics, Springer-Verlag, Berlin, 1975

21. R. N. Bracewell and J. A. Roberts, Australian J. Phys. 7, 615 (1954)

22. N. R. Hill and G. E. Ioup, J. Opt. Soc. Am. 66, 487 (1976)

23. R. N. Bracewell, The Fourier Transform and Its Applications, 2nd ed., McGraw-Hill, New York, 1978

24. E. O. Brigham, The Fast Fourier Transform, Prentice-Hall, 1974

25. J. W. Cooley and J. W. Tukey, Math. of Compt. 19, 297 (1965)

26. S. J. Howard, New Techniques in Fourier Deconvolution of Gas Chromatographic Data, Master's Thesis, University of Southern Mississippi, 1978

Publications

"The 127° Cylindrical Electrostatic Analyzer. I. Theory and Response Functions," Juliette W. Ioup, Grayson H. Rayborn, and George E. Ioup, submitted to Review of Scientific Instruments

"The 127° Cylindrical Electrostatic Analyzer. II. Effective Response Functions, Broadening and Output Curves," Juliette W. Ioup, submitted to Review of Scientific Instruments

Talks

"The 127° Cylindrical Electrostatic Analyzer," University of Southern Mississippi, Hattiesburg, 28 Jan 1977

"Distortion and Broadening of the 127° Cylindrical Electrostatic Analyzer," Louisiana Academy of Sciences, LSU-Shreveport, 5 Feb 1977

"The 127° Cylindrical Electrostatic Analyzer," University of New Orleans, 9 Feb 1977

Report on Summer Research Activities, NASA/ASEE Summer Faculty Fellowship Program, NASA-Langley Research Center, 4 Aug 1977

"Comparison of Theory and Experiment for Molecular Charge Exchange in Nitrogen," Louisiana Academy of Sciences, Nicholls State University, 4 Feb 1978

"Vibrational Excitation in H on H_2 Collisions," University of Southern Mississippi, Hattiesburg, 14 Apr 1978

Report on Summer Research Activities, NASA/ASEE Summer Faculty Fellowship Program, NASA-Langley Research Center, 1 Aug 1978

Report on Summer Research Activities, Instrument Research Division, NASA-Langley Research Center, 7 Aug 1978

Report on Summer Research Activities, Instrument Research Division, NASA-Langley Research Center, 8 Aug 1979

"The Quadrupole Mass Spectrometer," Loyola University, New Orleans, LA, 25 Sept 1979

Conference

"Introduction to Microcomputers and Microprocessors," NSF Chautauqua Short Course for College Teachers, 15-16 Nov 1979 and 21-22 Feb 1980, University of Texas at Austin

Books Purchased Under NASA Grant NSG 1361

P.Dahl, Introduction to Electron and Ion Optics, Academic Press, 1973

P. H. Dawson, ed., Quadrupole Mass Spectrometry and Its Applications, North Holland, 1976

F. O. Goodman and H. Y. Wachman, Dynamics of Gas-Surface Scattering, Academic Press, 1976

P. W. Hawkes, Quadrupoles in Electron Lens Design, Academic Press, 1970

H. Massey, Atomic and Molecular Collisions, Halstead, 1979

M. Prutton, Surface Physics, Clarendon, 1975

A. Septier, ed., Focusing of Charged Particles, Vol. I, Academic Press, 1967

J. R. Woodyard, Low Energy Sputtering Studies, Ph.D. Dissertation, University of Delaware, 1966

Equipment Purchased Under NASA Grant NSG 1361

HP 72221A Graphics Plotter
HP 72221A Buffer Expansion
HP PLOT/21 Graphics Software

Hazeltine 1410 Cathode Ray Tube Terminal
Acoustic Coupler

Tektronix 4006-1 Graphics Terminal
Tektronix Graphics Software